Neodymium and erbium coordination environments in phosphate glasses

M. Karabulut,* G. K. Marasinghe,[†] E. Metwalli,[‡] A. K. Wittenauer, and R. K. Brow[§]
Graduate Center for Materials Research, University of Missouri–Rolla, Rolla, Missouri 65401

C. H. Booth and D. K. Shuh
Chemical Sciences Division, The Glenn T. Seaborg Center, Lawrence Berkeley National Laboratory, Berkeley, California 94720
(Received 1 June 2001; revised manuscript received 30 October 2001; published 1 March 2002)

The local structures of Nd^{3+} and Er^{3+} ions in two series of rare-earth (RE) phosphate glasses with nominal compositions $xR_2O_3\text{-}(1-x)P_2O_5$, where $R=$ Nd and Er and $0.05 \leqslant x \leqslant 0.28$, have been characterized by L_{III}-edge extended x-ray-absorption fine-structure spectroscopy (EXAFS). The RE coordination number depends on the R_2O_3 content, decreasing from 9.0 (10) oxygen nearest neighbors in ultraphosphate compositions ($x<0.15$) to 6.4 (9) oxygen nearest neighbors for the metaphosphate ($x\sim0.25$) compositions. The average Er-O bond distance decreases from 2.29 (1) to 2.23 (1) Å, and the average Nd-O bond distance decreases from 2.40 (1) to 2.37 (1) Å over the same compositional range. The changes in coordination environments are consistent with the conversion of isolated RE polyhedra to clustered RE polyhedra sharing common oxygens as the number of available terminal oxygens per RE ion decreases with increasing x.

I. INTRODUCTION

Structural information about the local environments of rare-earth ions in phosphate glasses is useful because of the importance of these materials in optical and optoelectronic technologies.[1] For example, the coordination environments of the rare-earth ions affect the optical gain of an amplifier glass. Electric dipole coupling between neighboring excited RE ions leads to concentration quenching by a cooperative up-conversion process that results in the loss of an excited ion.[2] Nonradiative de-excitation can occur if one of the excited RE ions is coupled with an –OH impurity.[3] Thus, detailed information about the local structural environment of RE ions is important for understanding the photoluminescence behavior of RE-containing glasses.[4]

Phosphate glasses with high concentrations (up to 25 mole %) of rare-earth ions also possess interesting luminescent and magnetic properties that can be utilized in a variety of optical, optoelectronic, and optomagnetic applications, including Faraday rotator modulators, optical isolators, fiber lasers, etc.[5,6] Rare-earth metaphosphate (25 mole % R_2O_3) glasses exhibit unusual low-temperature thermal and acoustic properties that also depend on details of their short-range structures.[7–9]

The structure of simple phosphate glasses is dependent on composition, and can be classified by [O]:[P] ratios and relative fractions of Q^i phosphate tetrahedra, where i represents the number of neighboring P tetrahedra linked through common bridging oxygens.[10] A single-component P_2O_5 glass has [O]:[P]=2.5, and the glass possesses a structure based on a three-dimensional network of interconnected Q^3 tetrahedra. With the addition of a second oxide, (e.g., R_2O_3), bridging oxygens (P-O-P) are replaced by nonbridging oxygens (P-O-R) to form an ultraphosphate network ([O]:[P]<3.0) based on Q^2 and Q^3 tetrahedra. At the metaphosphate stoichiometry $(0.25R_2O_3 \cdot 0.75P_2O_5$, [O]:[P]=3.0), Q^2 tetrahedra link to form chains and rings, which themselves are tied together by the more ionic P-O-R^{3+}-O-P bonds. Further in-

creases in R_2O_3 content (>25 mole %) produce shorter polyphosphate chains that are terminated by Q^1 tetrahedra.

The coordination environments of monovalent and divalent metal ions in simple phosphate glasses also depend on composition. Hoppe and co-workers observed higher coordination numbers for these modifiers in ultraphosphate compositions that possess greater numbers of terminal oxygens (TO's) per modifier ion.[11,12] (Terminal oxygens include double-bonded oxygens associated with Q^3 tetrahedra and "nonbridging" oxygens on Q^2 tetrahedra that neutralize the modifier ions.) An increase in the metal-oxide content of the glass decreases the number of TO's available to coordinate the individual modifier ions and the average coordination number decreases accordingly. Changes in alkali coordination environments can be related to the compositional dependencies of the properties of binary ultraphosphate glasses.[13,14]

There have been a number of studies on the structure of binary rare-earth phosphate glasses with compositions near the metaphosphate stoichiometry $(0.17>R_2O_3>0.26)$.[15–24] Raman spectroscopy reveals that the addition of R_2O_3 to a binary phosphate glass creates terminal oxygens on progressively shorter phosphate chains, as expected from the increase in [O]:[P] ratio.[15,19] A neutron-diffraction study of a La-metaphosphate glass indicated that the average La-polyhedra includes 7.0 (5) oxygen nearest neighbors,[20] whereas the Eu polyhedra in a Eu-metaphosphate glass possesses ~6 oxygen nearest neighbors.[25] Extended x-ray absorption fine structure (EXAFS) studies of RE phosphate glasses with metaphosphate compositions identified first shell R-O coordination numbers ranging from 5.5 (5) to 10.4 (27).[21,22] Lower coordination numbers and shorter average R-O bond lengths were found for rare-earth ions with greater atomic numbers ($Z>64$), a consequence of the lanthanide contraction effect.

Less is known about the structures of RE ultraphosphate glasses ($x<0.25$). Mountjoy *et al.* recently reported an EXAFS study of RE coordination numbers in several different ultraphosphate compositions, with R_2O_3 contents in the

TABLE I. Compositions and densities of Nd and Er phosphate glasses examined in this study.

Batched	Analyzed composition (mole %)	Density (g/cm^3)
$5Nd_2O_3$-$95P_2O_5$	$6.6Nd_2O_3$-$89.8P_2O_5$-$3.5SiO_2$	2.51
$10Nd_2O_3$-$90P_2O_5$	$8.0Nd_2O_3$-$82.9P_2O_5$-$9.1SiO_2$	2.68
$15Nd_2O_3$-$85P_2O_5$	$15.0Nd_2O_3$-$83.1P_2O_5$-$1.9SiO_2$	2.87
$25Nd_2O_3$-$75P_2O_5$	$25.4Nd_2O_3$-$72.4P_2O_5$-$2.2SiO_2$	3.15
$5Er_2O_3$-$95P_2O_5$	$4.9Er_2O_3$-$92.3P_2O_5$-$2.8SiO_2$	2.60
$10Er_2O_3$-$90P_2O_5$	$8.1Er_2O_3$-$87.9P_2O_5$-$4.0SiO_2$	2.63
$15Er_2O_3$-$85P_2O_5$	$18.8Er_2O_3$-$76.0P_2O_5$-$5.2SiO_2$	2.65
$25Er_2O_3$-$75P_2O_5$	$27.7Er_2O_3$-$72.3P_2O_5$-$0.0SiO_2$	3.58

range 0.187–0.235.[24] They found RE coordination numbers near six, similar to those found in earlier studies of RE metaphosphate glasses. There was no evidence of the expected increase in RE coordination numbers for the ultraphosphate compositions, despite the observation that the number of RE oxygen nearest neighbors increases from six in the structures of crystalline RE metaphosphates (RP_3O_9) to eight in crystalline RE ultraphosphates (RP_5O_{14}).[26,27]

In the present study, we have also used EXAFS to determine the average local bonding environments of Nd^{3+} and Er^{3+} ions in two series of phosphate glasses. We have examined a much broader range of compositions ($0.05 \leqslant$ mole fraction $R_2O_3 \leqslant 0.28$) than in previous studies, and we find that the average RE coordination number decreases with increasing R_2O_3 content. The RE coordination numbers can be explained by a structural model that involves the compositional dependence of the number of terminal oxygens per R^{3+} ion.

II. EXPERIMENTAL PROCEDURES

A. Sample preparation

Ultraphosphate glasses were prepared from mixtures of P_2O_5 (purified by vacuum sublimation) and either reagent grade $NdPO_4$ or $ErPO_4$. Ultraphosphate melts ($0.05 \leqslant x \leqslant 0.20$) were processed in sealed silica ampoules to avoid P_2O_5 volatilization.[13] Raw materials were handled in an argon drybox before being sealed in flame-dried silica ampoules. These samples were then heated to 1000–1200 °C, depending on the composition, and held for about 30 min until a homogeneous liquid was formed. The ampoules were removed from the furnace and immediately transferred to the drybox to avoid exposing the resulting glasses to the ambient. Each metaphosphate ($x = 0.25$) composition was melted in open silica crucibles at 1400 °C in air. The composition of each glass was determined using an analytical scanning electron microscope.[28] At least five spots were examined on each sample and the average is reported in Table I. These analyses were reproducible to $\pm 5\%$. Densities were determined by Archimedes' method, using kerosene as the buoyancy fluid. At least three samples of each composition were analyzed, and the average value (± 0.010 g/cm^3) is reported.

NdP_5O_{14} and ErP_5O_{14} crystals were grown from solution and used as reference materials for EXAFS experiments.

About 1 g of Nd_2O_3 (99.9999%) or Er_2O_3 (99.9999%) was added to 30 mL of 85% phosphoric acid in an amorphous carbon crucible and the solution was gradually heated to 450 °C and held for 10 days. After cooling and removing residual phosphoric acid by washing several times with distilled water, thin platelets of NdP_5O_{14} and ErP_5O_{14}, several millimeters long, were obtained.

B. EXAFS experiments and data analysis

Room-temperature L_{III} edge EXAFS spectra were collected at the Stanford Synchrotron Radiation Laboratory on beamline 4-1 using a half-tuned Si(220) double-crystal monochromator. Powders from each glass were mixed with polystyrene beads, and loaded into an aluminum holder with kapton windows. Samples were prepared in an argon drybox, and transferred to the EXAFS station in sealed containers. All EXAFS spectra were taken in transmission mode. In general, 3–4 scans to $k = 9$–12 Å^{-1} were averaged for each glass to obtain a suitable signal-to-noise ratio. All spectra were energy calibrated by simultaneously measuring the absorption spectrum from respective reference materials. EXAFS spectra from NdP_5O_{14} and ErP_5O_{14} crystals were also collected to compare and use in fitting the glass data.

In the EXAFS analysis, the oscillatory fine structure above the absorption edge, due primarily to the scattering of the photoelectron off near neighbor atoms, is utilized. The amplitude of the EXAFS function χ is proportional to the number of near neighbors, and the change of phase with the wavelength of the photoelectron depends on the distance between the emitter and the backscattering atom. The backscattering strength also depends on the atoms involved in the backscattering process.[29–31]

EXAFS data reduction was carried out by standard methods described elsewhere[29–32] using the suite of programs EXAFSPAK. The EXAFS function $\chi(E)$ is calculated from the absorption data using $\chi(E) = [\mu(E) - \mu_0(E)]/\mu_0(E)$, where the absorption coefficient $\mu_0(E)$ is the so-called "embedded-atom" absorption, which does not include EXAFS oscillations, and $\mu(E)$ includes absorption from the edge of interest and the EXAFS oscillations. The background is removed from $\chi(E)$ by fitting the pre-edge with a polynomial function such that the background subtracted absorption above the edge follows the Victoreen formula.[29–32] $\chi(E)$ is

then recalculated into k space using $k = [2m(E-E_0)]^{1/2}/\hbar$ and $\mu_0(E)$ is isolated by fitting a spline function to the data above the absorption edge. Fits to $\chi(k)$ use theoretical back-scattering phase and amplitude functions for the various scattering paths, as calculated by FFEF7,[33] on appropriate model compounds as described below.

Double-electron excitation (DEE) may contribute to the x-ray-absorption background for the rare-earth L_{III} edge EXAFS spectra. This effect was reported, to varying degrees, between $k=5$ and 7 Å^{-1} in the EXAFS spectra of some RE-phosphate glasses, producing peaks in the radial distribution functions that may distort the fits to first correlation peaks corrected by simple Fourier filtering methods.[21–24] These peaks are found near ~ 1.8 Å in some of the Fourier transforms (FT) spectra collected in the present study, but their magnitudes are small and these effects do not significantly alter the analysis of the first correlation peak. Fitting the $k^3\chi$ data instead of the $k\chi$ data also reduces the effects of DEE. The EXAFS and FT spectra of the 15Nd85P glass in this study are comparable to reported spectra[22] adjusted for DEE collected from a similar glass. For these reasons, the spectra in the present study were not adjusted to account for the effects of double-electron excitation.

III. RESULTS

A. Glass formation

Clear, homogeneous glasses could be prepared in both $xR_2O_3\cdot(1-x)P_2O_5$ systems in the range (as batched) $0.05 \leq x \leq 0.25$. The analyzed R:P ratios of the glasses prepared in both sealed ampoules and open crucibles were similar to the batched compositions (Table I). However, the glasses also contain 2–10-mole % SiO_2, picked up from the silica ampoule or crucible during melt preparation. Glasses melted at higher temperatures and for longer times have larger silica contents. The glass densities are given in Table I. For both systems, density increases with R_2O_3 content.

B. EXAFS results

1. Crystalline NdP_5O_{14} and ErP_5O_{14}

Figure 1 shows the k^3-weighted EXAFS and corresponding Fourier transforms (thin lines) and the theoretical fits (heavy lines) for the NdP_5O_{14} and ErP_5O_{14} crystals. The available **k** range was larger for the Er L_{III} edge than for the Nd L_{III} edge, since the Er L_{II}-edge interference is located at larger **k** relative to the L_{III}-edge absorption. An amplitude reduction factor of 0.75 was obtained from these fits, and is used as a fixed parameter for subsequent fits of the glass spectra described below. This amplitude reduction factor is similar to that used elsewhere for RE metaphosphate glasses.[21,22]

Diffraction studies indicate that the near neighbor environments around the RE ions for both of these crystalline materials is complex. There are eight oxygen atoms surrounding the Nd atom at seven different distances, ranging from 2.38 (1) to 2.50 (1) Å, in the structure of crystalline NdP_5O_{14}.[26] There are also eight oxygen atoms surrounding
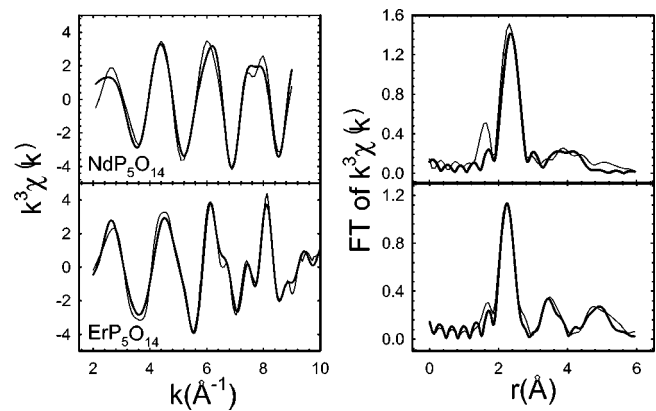

FIG. 1. EXAFS (left) and corresponding Fourier transform (right) spectra for crystalline NdP_5O_{14} and ErP_5O_{14}. The thin lines are the experimental data, and the heavy lines are the theoretical fits.

each Er atom at eight different distances, ranging from 2.27 (1) to 2.38 (1) Å, in the structure of ErP_5O_{14}.[27] The individual R-O distances cannot be isolated from our EXAFS data. However we can consider average R-O distances for the crystals and glasses. Fits to the EXAFS from crystalline NdP_5O_{14} yield an Nd-O coordination number of 8.8 (20) with average Nd-O distance of 2.43 (1) Å, compared to the coordination number (CN) of 8 and an average Nd-O distance of 2.44 (1) Å obtained by x-ray diffraction.[26] Mountjoy et al.[24] reported a Nd CN of 8.0 (7) and an average Nd-O bond length of 2.44 (1) Å in their EXAFS study of NdP_5O_{14}. Fits to the EXAFS from ErP_5O_{14} yield an Er-O CN of 8.6 (7) with an average distance of 2.34 (1) Å, compared with a CN of 8 and an average Er-O distance of 2.33 (1) Å obtained by diffraction.[27] In general, CN's from the EXAFS experiments are about 10% higher than those reported from diffraction studies, whereas the *average R*-O distance is in agreement within 0.01 Å. The uncertainties associated with the EXAFS-derived coordination numbers are greater than those from x-ray diffraction measurements.

2. Nd and Er phosphate glasses

The k^3-weighted EXAFS and corresponding FT's for Nd and Er phosphate glasses are shown in Figs. 2 and 3, respectively. The theoretical fits are given as thick lines in both figures. The structural parameters obtained from the EXAFS fits to the Nd- and Er-data sets are summarized in Tables II and III, respectively. The errors associated with each result and fitting parameter (given in parentheses) are 95% confidence limits calculated by EXAFSPAK. For both series of glasses, fits that include three shells were performed: the R-O and R-P first-shell correlations and a second R-O shell correlation. [Because of the poor quality of the EXAFS data for the $5Nd_2O_3$-$95P_2O_5$ (mole %) glass, only a first Nd-O shell fit was performed.] For the Nd series, in the first shell, the oxygen CN is close to 9.0 (10) for glasses containing up to ~ 15 mole % Nd_2O_3. The Nd CN decreases to 6.4 (9) for the Nd metaphosphate glass (~ 25 mole % Nd_2O_3). Nd-O distances in the first coordination shell decrease slightly, from 2.40 (1) to 2.37 (1) Å, over the entire compositional range.

FIG. 2. EXAFS and corresponding Fourier transforms for Nd phosphate glasses. The heavy lines are the theoretical fits.
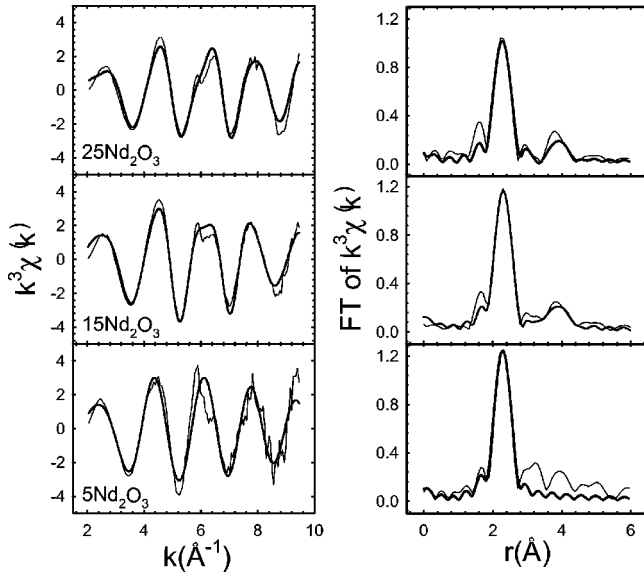

FIG. 3. EXAFS and corresponding Fourier transforms for Er phosphate glasses. The heavy lines are the theoretical fits.

Similar trends are observed for the Er phosphate glasses. The average coordination number decreases from 8.3 (20) to 6.3 (6) when the Er_2O_3 content increases from 4.9 to 27.7 mole %. The average Er-O distance decreases from 2.29 (1) Å to 2.23 (1) Å over the same range. Figure 4 shows the decrease in Nd and Er coordination numbers with increasing rare earth oxide contents.

The average Nd- and Er-coordination environments determined in the present EXAFS studies and summarized in Tables II and III, respectively, can be compared to those reported in previous EXAFS studies of "near metaphosphate" compositions. For example, EXAFS spectra collected at 80 K from a Nd-phosphate glass with 18.7 mole % Nd_2O_3 ($x=0.187$) glass indicate a Nd CN of 5.4 (4) and an average Nd-O bond-length of 2.37 (1) Å.[24] An earlier EXAFS study of the same sample indicated an average Nd CN closer to 8.[22] An x-ray scattering study of this glass indicates a Nd CN of 6.4 (6) and a Nd-O bond length of 2.36 (2) Å.[34] An EXAFS study of a $0.24Er_2O_3$-$0.76P_2O_5$ glass indicates an Er-O distance of 2.22 (1) Å and a CN of 5.7 (4),[22] compared to an Er-O bond distance and Er CN of 2.23 (1) Å and 6.6 (5), respectively, determined by x-ray scattering.[34]

Both the Nd and Er phosphate glasses have phosphorus neighbors in the second coordination shell, with Nd-P and Er-P CN's ranging from 2.5 (7) to 3.9 (9). The Nd-P dis-
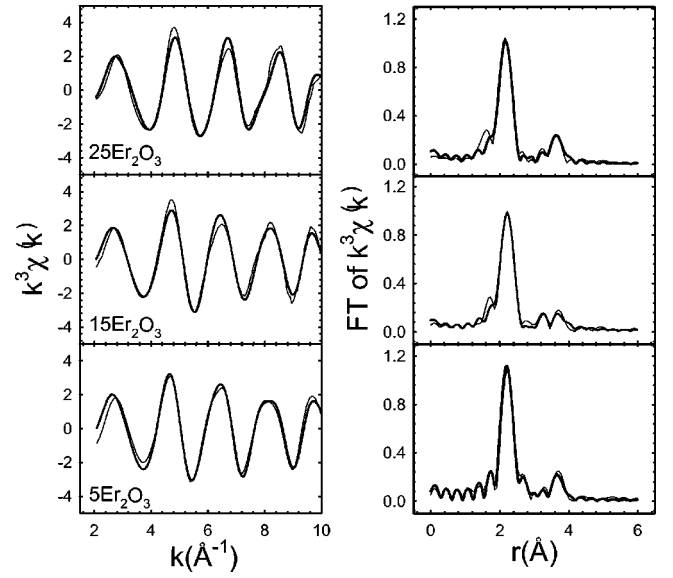
tances are close to 3.85 (2) Å, and the Er-P distances are 3.52 (2) Å. These distances compare favorably to those distances calculated by us using the reported crystal structures:[26,27] 3.70 and 3.76 Å, for NdP_5O_{14} and NdP_3O_9, respectively, and 3.59 and 3.48 Å for ErP_5O_{14} and ErP_3O_9, respectively. The third shell consists of oxygen neighbors with average distances of 4.5 (3) Å and 3.75 (3) Å for Nd and Er phosphate glasses, respectively. The greater errors associated with the CN's in the third shell reflect the decrease in EXAFS resolution at greater distances and the contributions from multiple-scattering processes.[24] Attempts were made to include R-R scattering up to 4.5 Å but there was no fit convergence for any EXAFS data.

IV. DISCUSSION

Previous structural studies of lanthanide phosphate glasses characterized the changes in the phosphate network as the lanthanide content is increased.[19,35,36] In general, the structures convert from the Q^3/Q^2 phosphate networks associated with ultraphosphate compositions to the chainlike structures of metaphosphate and polyphosphate compositions.[10] As noted in Sec. I, there were many recent studies of the local structural arrangements of R^{3+} ions in

TABLE II. Structural parameters (coordination number N, bond distance r, and Debye-Waller factor σ) for Nd-P glasses obtained from Nd L_{III}-edge EXAFS fits. The errors given in parentheses are 95% confidence limits given by EXAFSPAK. An amplitude reduction function of $S_0^2=0.75$ was used for fitting the experimental results.

Sample	5Nd-95P			10Nd-90P			15Nd-85P			25Nd-75P		
Shell	N	$r(Å)$	$\sigma(Å)$	N	$r(Å)$	$\sigma(Å)$	N	$r(Å)$	$\sigma(Å)$	N	$r(Å)$	$\sigma(Å)$
Nd-O	9.2 (10)	2.40 (1)	0.08 (3)	8.4 (10)	2.38 (2)	0.08 (3)	9 (1)	2.40 (1)	0.09 (2)	6.4 (9)	2.37 (1)	0.07(2)
Nd-P	—	—	—	2.5 (9)	3.84 (3)	0.08 (2)	3.7 (10)	3.85 (2)	0.09 (5)	2.2 (9)	3.87 (3)	0.08 (3)
Nd-O	—	—	—	11 (5)	4.5 (4)	0.10 (5)	9 (3)	4.54 (3)	0.10 (5)	9 (4)	4.54 (3)	0.12 (7)

TABLE III. Structural parameters (coordination number N, bond distance r, and Debye-Waller factor σ) for Er-P glasses obtained from Er L_{III}-edge EXAFS fits. The errors given in parentheses are 95% confidence limits given by EXAFSPAK. An amplitude reduction function of $S_0^2 = 0.75$ was used for fitting the experimental results.

| Sample | 5Er-95P | | | 10Er-90P | | | 15Er-85P | | | 25Er-75P | | |
Shell	N	r(Å)	σ(Å)	N	r(Å)	σ(Å)	N	r(Å)	σ(Å)	N	r(Å)	σ(Å)
Er-O	8.3 (20)	2.29 (1)	0.08 (3)	8.8 (10)	2.30 (1)	0.09 (3)	7.3 (4)	2.29 (1)	0.08 (2)	6.3 (6)	2.23 (1)	0.08(2)
Er-P	2.8 (8)	3.78 (2)	0.08 (3)	2.4 (6)	3.57 (3)	0.10 (2)	2.5 (7)	3.53 (3)	0.08 (2)	3.9 (1)	3.51 (3)	0.13 (6)
Er-O	—	—	—	3.7 (9)	3.79 (2)	0.09 (3)	2.5 (8)	3.74 (3)	0.07 (2)	2.3 (7)	3.76 (2)	0.06 (1)

lanthanide phosphate glasses, but none indicated the changes in the RE coordination environments seen in the present work.

The dependence of RE coordination environments on the R_2O_3 contents in phosphate glasses can be understood by considering the structures of RE phosphate crystals. Isolated, eight-coordinated RE polyhedra are found in RE ultraphosphate (RP_5O_{14}) crystals.[26,27] Terminal oxygens from both Q^2 and Q^3 phosphate tetrahedra comprise the local coordination environments of these R^{3+} ions. There are two crystalline RE-metaphosphate (RP_3O_9) polymorphs.[37] In the orthorhombic form, distorted RE polyhedral clusters link the metaphosphate anions through terminal oxygens on Q^2 tetrahedra. Eight oxygens, two of which are common to neighboring RE polyhedra through slightly longer R-O bonds, coordinate these 6+2 polyhedra. Distorted, isolated RE octahedra are found in the lower-density monoclinic forms that are more common for smaller, higher atomic number rare earth ions.

Hoppe *et al.* argued that the bonding arrangements in phosphate glasses are similar to those in phosphate crystals, and they proposed that the structures and properties of ultraphosphate glasses depend on the number of terminal oxygens available to coordinate the modifier ions.[11,12,20] For glasses with the stoichiometry $x(M_{2/v}O) \cdot (1-x)P_2O_5$, where M is a

metal modifier and v is the valence of the modifier ion, the number of terminal oxygens per modifying ion is $M_{TO} = v(1/x)$.[11] This equation can be rewritten for $xR_2O_3 \cdot (1-x)P_2O_5$ glasses to determine the dependence of the number of terminal oxygens per R^{3+} ion (TO/R^{3+}) on the mole fraction (x) of R_2O_3:

$$TO/R^{3+} = (1+2x)/x. \quad (1)$$

Hoppe noted that there are two structurally sensitive compositional ranges that depend upon the modifier coordination number (CN_M) and the number of terminal oxygens (M_{TO}).[15] When $M_{TO} > CN_M$, there are sufficient terminal oxygens available to bond with each modifier ion, and these ions can then exist as isolated coordination polyhedra within the phosphate network, as is the case for crystalline NdP_5O_{14} and ErP_5O_{14}. When $M_{TO} < CN_M$, there are not enough terminal oxygens available to satisfy the coordination requirements of *isolated* modifier ions, and thus these ions must cluster to share the available terminal oxygens through M-O-M linkages between modifier coordination polyhedra. Such polyhedral clusters link neighboring Q^2 anions, as found in the orthorhombic forms of crystalline RP_3O_9. The transition from the first compositional region to the second has a pronounced effect on the properties of binary ultraphosphate glasses, including the densities and refractive indices of La-phosphate glasses.[36]

The present EXAFS results (Fig. 4) indicate that there is a decrease in the average RE coordination number (and a reduction in the average R-O bond length) with increasing R_2O_3 content for Nd and Er glasses. According to Eq. (1), *isolated* eight-coordinated R^{3+} ions, like those found in the RP_5O_{14} crystals, can exist in $xR_2O_3 \cdot (1-x)P_2O_5$ glasses when $x \leq 0.167$. *Isolated* RE polyhedra can also exist in glasses with greater R_2O_3 contents only if the average RE coordination number decreases. The solid line in Fig. 4 is the predicted dependence according to Eq. (1). Note that for coordination numbers and compositions to the left of (and below) the line, isolated polyhedra are expected to be present. Clustered RE polyhedra sharing common terminal oxygens will result for CN and composition combinations to the right of (and above) the line. The decreases in Nd- and Er- CN's thus, at least initially, avoid the formation of RE clusters in glasses with increasing R_2O_3. Note that Eq. (1) predicts that when R_2O_3 exceeds 25 mole %, the CN must fall below six in order for the RE polyhedra to remain isolated. It is unlikely that these large ions possess coordination numbers under six,[38] and so RE clusters are expected to be present in
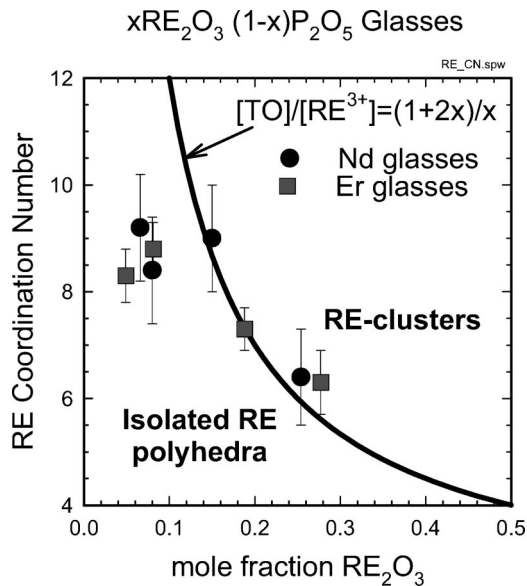

xRE$_2$O$_3$ (1-x)P$_2$O$_5$ Glasses

FIG. 4. The dependence of Er and Nd coordination numbers on composition. The solid line is based on Eq. (1).

glasses with R_2O_3 contents >25 mole %. Similar results were obtained and similar conclusions drawn from a recent high-energy x-ray scattering study of La ultraphosphate glasses.[39]

The RE coordination numbers are plotted in Fig. 4 against the analyzed R_2O_3 mole fractions that include the silica impurities (Table I). Silica incorporation can affect the quantitative relationship between RE CN's and R_2O_3 content in two ways, depending on its affect on the glass structure. If silica is incorporated in separate, silica-rich regions, then the number of terminal oxygens per R^{3+} ion will depend only on the R/P ratio, and the individual data points would be shifted to the right in silica-free glasses. (For the glass with the greatest silica content, $8.0Nd_2O_3 \cdot 82.9P_2O_5 \cdot 9.1SiO_2$, the shift would be from 8.0 to 8.8 mole % Nd_2O_3.) If silica bonds through terminal oxygens on phosphate tetrahedra to form the $SiO_6{}^{2-}$ species found when silica is added to a metaphosphate glass,[40] then the line in Fig. 4 representing Eq. (1) should be shifted to the left to account for the reduction in available terminal oxygens to coordinate individual RE polyhedra. In either case, however, the relatively small concentrations of silica in these glasses do not lead to significant changes in the CN vs R_2O_3 relationships for the two series of glasses and so the quantitative explanation for the CN decrease for R_2O_3 contents over 16.7 mole % remains valid.

V. SUMMARY

EXAFS indicates that the average coordination environments of Nd^{3+} and Er^{3+} ions in rare-earth phosphate glasses depend on the glass composition and can be understood in terms of the number of terminal oxygens available from the phosphate network to satisfy the rare-earth coordination requirements. In glasses with Nd_2O_3 and Er_2O_3 contents lower than the 16.7 mole % found in the crystalline ultraphosphates (RP_5O_{14}), there are sufficient terminal oxygens to create isolated RE polyhedra with large coordination numbers (8–9). Increasing the R_2O_3 contents to ~ 25 mole % reduces the number of available terminal oxygens per R^{3+} ion and the average Nd^{3+} and Er^{3+} coordination numbers accordingly decrease to ~ 6. The lower RE coordination numbers make it possible for isolated rare earth polyhedra to still exist in R_2O_3-rich glasses.

*Present address: Department of Physics, University of Kafkas, Kars, Turkey.

†Present address: Department of Physics, University of North Dakota, Grand Forks, ND 58202.

‡Present address: National Research Center, Glass Research Dept., Dokki, Cairo, Egypt.

§Corresponding author. Email address: brow@umr.edu

[1] M. J. Weber, *Materials Science and Technology, A Comprehensive Treatment*, edited J. Zarzycki (VCH, Weinheim, 1991), Vol. 9, p. 654.

[2] F. Auzel, J. Lumin. **45**, 341 (1990).

[3] Y. Yan, A. J. Faber, and H. de Waal, J. Non-Cryst. Solids **181**, 283 (1995).

[4] P. M. Peters and S. N. Houde-Walter, J. Non-Cryst. Solids **239**, 162 (1998).

[5] M. M. Broer, A. J. Bruce, and W. H. Grodkiewicz, Phys. Rev. B **45**, 7077 (1992).

[6] H. P. Weber, T. C. Damen, H. G. Danielmeyer, and B. C. Tofield, Appl. Phys. Lett. **22**, 534 (1973).

[7] A. Mierzejewski, G. A. Saunders, H. A. A. Sidek, and B. Bridge, J. Non-Cryst. Solids **104**, 323 (1988).

[8] H. M. Farok, G. A. Saunders, W. C. K. Poon, J. Crain, H. Vass, W. Hönle, and E. Schöner, J. Mater. Sci. **34**, 2389 (1999).

[9] A. Fontana, G. Carini, A. Brodin, L. M. Torell, M. Börjesson, and G. A. Saunders, Philos. Mag. **71**, 525 (1995).

[10] R. K. Brow, J. Non-Cryst. Solids **263-264**, 1 (2000).

[11] U. Hoppe, J. Non-Cryst. Solids **195**, 138 (1996).

[12] U. Hoppe, G. Walter, R. Kranold, D. Stachel, and A. Barz, J. Non-Cryst. Solids **192-193**, 28 (1995).

[13] J. J. Hudgens and S. W. Martin, J. Am. Ceram. Soc. **76**, 1691 (1993).

[14] R. K. Brow, C. A. Click, and T. M. Alam, J. Non-Cryst. Solids **274**, 9 (2000).

[15] K. Sun and W. M. Risen, Jr., Solid State Commun. **60**, 697 (1986).

[16] H. Ebendorff-Heidepriem, D. Ehrt, M. Bettinelli, and A. Speghini, J. Non-Cryst. Solids **240**, 66 (1998).

[17] H. Ebendorff-Heidepriem and D. Ehrt, Glasstech. Ber. Glass. Sci. Technol. **71**, 289 (1998).

[18] T. Brennan, J. C. Knight, and G. A. Saunders, Phys. Chem. Glasses **40**, 113 (1999).

[19] S. H. Morgan, R. H. Magruder, and E. Silberman, J. Am. Ceram. Soc. **70**, C378 (1987).

[20] U. Hoppe, R. Kranold, D. Stachel, A. Barz, and A. C. Hannon, J. Non-Cryst. Solids **232-234**, 44 (1998).

[21] D. T. Bowron, G. A. Saunders, R. J. Newport, B. D. Rainford, and H. B. Senin, Phys. Rev. B **53**, 5268 (1996).

[22] R. Anderson, T. Brennan, J. M. Cole, G. Mountjoy, D. M. Pickup, R. J. Newport, and G. A. Saunders, J. Mater. Res. **14**, 4706 (1999).

[23] D. T. Bowron, R. J. Newport, B. D. Rainford, G. A. Saunders, and H. B. Senin, Phys. Rev. B **51**, 5739 (1995).

[24] G. Mountjoy, J. M. Cole, T. Brennan, R. J. Newport, G. A. Saunders, and G. W. Wallidge, J. Non-Cryst. Solids **279**, 20 (2001).

[25] M. Cannas, E. Manca, G. Pinna, A. Speghini, and M. Bettinelli, Z. Naturforsch. **53A**, 919 (1998).

[26] H. Y.-P. Hong, Acta Crystallogr., Sect. B: Struct. Crystallogr. Cryst. Chem. **30**, 468 (1974).

[27] B. J. Trzebiatowska and Z. Mazurak, Acta Crystallogr., Sect. B: Struct. Crystallogr. Cryst. Chem. **36**, 1639 (1980).

[28] Hitachi S4700 field emission scanning electron microscope with EDAX Phoenix Microanalysis System.

[29] B. K. Teo, *EXAFS*: *Basic Principles and Data Analysis* (Springer, Berlin, 1986).

[30] *X-ray Absorption: Principles, Applications, Techniques of EXAFS, SEXAFS, and XANES*, edited by R. Prins and D.E. Koningsberger (Wiley-Interscience, New York, 1988).

[31] G. E. Brown, Jr., G. Calas, G. A. Waychunas, and J. Petiau, in *Reviews In Mineralogy*, edited by F. C. Hawthorne, (Mineralogical Society of America, Washington, DC, 1995) Vol. 32, p. 431.

[32] M. Karabulut, G. K. Marasinghe, C. S. Ray, D. E. Day, G. D. Waddill, C. H. Booth, J. J. Bucher, D. L. Caulder, D. K. Shuh, P. G. Allen, and M. Grimsditch, J. Mater. Res. **15**, 1972 (2000).

[33] S. I. Zabinsky, A. Ankudinov, J. J. Rehr, and R. C. Albers, Phys. Rev. B **52**, 2995 (1995).

[34] J. M. Cole, E. R. H. van Eck, G. Mountjoy, R. Anderson, T. Brennan, G. Bushnell-Wye, R. J. Newport, and G. A. Saunders, J. Phys.: Condens. Matter **13**, 4105 (2001).

[35] K. Sun and W. M. Risen, Jr., Solid State Commun. **60**, 697 (1986).

[36] R. K. Brow, E. Metwalli, and D. L. Sidebottom, Inorganic Optical Materials II, Proceedings of the 45th Annual Meeting of the SPIE, 2000, Vol. 4102, p. 88.

[37] M. Cannas, E. Manca, G. Pinna, M. Bettinelli, and A. Speghini, Z. Naturforsch. **53A**, 919 (1998).

[38] R. D. Shannon, Acta Crystallogr., Sect. A: Cryst. Phys., Diffr., Theor. Gen. Crystallogr. **32**, 751 (1976).

[39] U. Hoppe, E. Metwalli, R. K. Brow, and J. Neuefeind, J. Non-Cryst. Solids **297**, 263 (2002).

[40] R. Dupree, D. Holland, M. G. Mortuza, J. A. Collins, and M. W. G. Lockyer, J. Non-Cryst. Solids **106**, 18 (1988).